SYNTHESIS, SPECTRAL CHARACTERIZATION, AND BIOLOGICAL EVALUATION OF SOME LANTHANIDE(III) COMPLEXES OF SCHIFF BASES OF THIOCARBOHYDRAZIDE DERIVATIVES

Dr. Sharad Sankhe[1*,] and Mr. Pratik Sarvade[2]

[1*]Professor, Department of Chemistry, Patkar-Varde College, Goregaon West, Mumbai-62, India.
[2]PhD scholar, Department of Chemistry, Patkar-Varde College, Goregaon West, Mumbai-62, India.

*Corresponding Author: Dr. Sharad Sankhe
*Professor, Department of Chemistry, Patkar-Varde College, Goregaon West, Mumbai-62, India.

Abstract

Thiocarbohydrazide-derived α-benzilmonoximethiocarbohydrazie-*p*-bromobenzaldehyde (HBMT *p*BB) has been utilized to synthesize and characterize complexes with inner transition metals, namely La(III), Nd(III), Gd(III), Sm(III), Pr(III), Tb(III), Dy(III), Eu(III), Lu(III), and Ce(III). The structural and bonding properties of these complexes were investigated through various analytical techniques, including elemental analysis, physical conductivity measurements, and magnetic susceptibility measurements. Additionally, spectral analyses, encompassing PMR (proton magnetic resonance), FT(IR) (Fourier-transform infrared) Electronic absorption spectra and Powder XRD were employed to gain insights into the complex structures and their bonding nature.

The trivalent metal complexes, formed as a result of these reactions, exhibited a consistent seven-coordinate geometry. To further explore their potential applications, the prepared complexes were evaluated for their antifungal and antibacterial activities against four bacterial species. Specifically, the tested gram-positive strains included *B. subtilis* (MCC 2010) and *S. aureus* (MCC 2408), while the gram-negative strains encompassed *P. aeruginosa* (MCC 2080) and *E. coli* (MCC 2412). These investigations aimed to shed light on the potential biological efficacy of the synthesized complexes against a diverse range of microorganisms

Keywords: Lanthanide complexes, α-benzilmonoxime, thiocarbohydrazide, *p*-bromobenzaldehyde

Introduction:

Thiocarbohydrazide holds significance as a pivotal class of drugs, with its reported application as the initial method for antimicrobial drug development [1-3]. The exploration of numerous derivatives of thiocarbohydrazide has led to the synthesis, characterization, and evaluation of their diverse pharmacological activities [4], including antitumor [5], antibacterial [6], hypoglycemic [7], anti-carbonic anhydrase [8], antithyroid [9], diuretic [10], and protein inhibitory properties [11]. The past decade has witnessed a surge in research and heightened interest in novel methodologies aimed at effectively combating bacteria and viruses associated with various ailments. Metal-based therapeutics have emerged as highly effective approaches for the treatment of such conditions, with the ability of metal ions to bind with peptides and proteins playing a crucial role in this context [12-15].

The allure of simple and N-substituted thiocarbohydrazide in metal-based therapy has intensified, inspired by the successful introduction of thiocarbohydrate metal complexes to thwart bacterial infections. These complexes, formed by trivalent metal ions, leverage the slow release of the metal ion from the source, a process intricately dependent on binding nature. The versatile chemistry of both thiocarbohydrazide and α-benzilmonoxime has prompted the exploration of their combined chemistry, unveiling intriguing biological and structural properties.

In the subsequent sections, we delve into the discussion of more complexes derived from thiocarbohydrazide and α-benzilmonoximethiocarbohydrazide-*p*-bromobenzaldehyde, along with their inner transition metal counterparts (La(III), Nd(III), Gd(III), Sm(III), Pr(III), Tb(III), Dy(III), Eu(III), Lu(III), and Ce(III)). The focus extends to unraveling their binding behavior and assessing their in vitro antifungal and antibacterial activities. This comprehensive exploration aims to contribute to the growing body of knowledge surrounding the potential therapeutic applications of these compounds in the realm of microbial infections and related health concerns.

**Experimental:**
Materials and Measurement:
All the essential initial substances were of high chemical purity, ensuring the integrity of the experimental procedures. The solvent employed for both spectral and physical measurements adhered to analytical reagent (AR) grade standards, guaranteeing a consistent and reliable medium for analysis. Lanthanide (III) salts were specifically utilized in the form of nitrates, contributing to the formation of the desired complexes.

Various analytical techniques, including FT(IR), PMR, electronic spectra, and elemental analyses encompassing C, H, N, S, and O, and Powder XRD were conducted using dedicated instruments. Magnetic and conductance measurements were also performed to gain insights into the inherent properties of the synthesized compounds.

The evaluation of in vitro antifungal, antibacterial and cytotoxic activities was carried out at the Rahul Dharkar College of Pharmacy and Research Institute, located in Karjat, Raigad, India. This comprehensive study aimed to assess the potential therapeutic efficacy of the synthesized compounds against fungal and bacterial strains, contributing valuable insights into their pharmacological applications. The meticulous selection of high-quality starting materials, coupled with rigorous analytical methodologies and biological assessments, underscores the robustness and reliability of the experimental framework employed in this research endeavor.

Synthesis of HBMT*p*BB ligand
A solution was prepared by combining α-benzilmonoximethiocarbohydrazide (10 mmol) with hot ethanol (50 ml), to which hot p-bromobenzaldehyde (12.5 mmol) in ethanol (50 ml) was added. The resulting reaction mixture underwent reflux for a duration of 5 hours to facilitate the chemical transformation. Subsequently, the reaction mixture was permitted to cool to room temperature, and the formed product was collected through filtration. To ensure the removal of impurities, the collected product was washed with hot distilled water and subsequently dried under vacuum conditions, utilizing anhydrous calcium chloride to enhance the efficiency of the drying process. This meticulous sequence of steps was undertaken to ensure the successful synthesis of the desired compound, highlighting the attention to detail and precision in the experimental protocol.
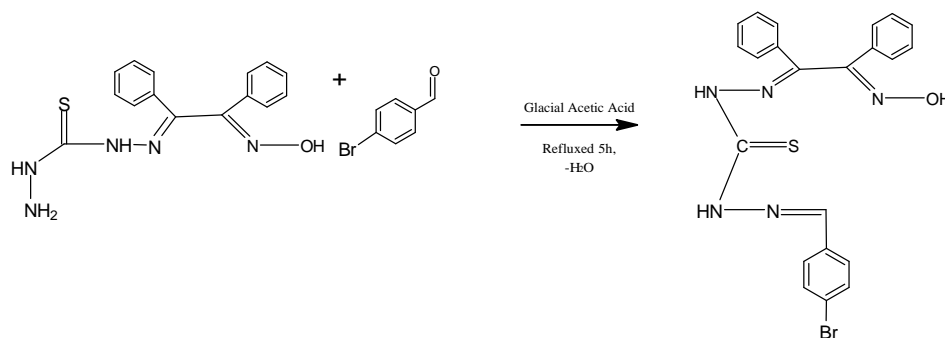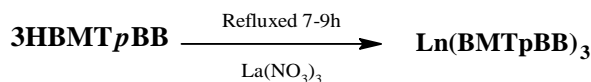
Scheme-I: Preparation of α-benzilmonoximethiocarbohydrazide-*p*-bromobenzaldehyde ligand

Preparation of metal complexes:

A solution composed of Ln(III)NO$_3$ (where Ln represents La(III), Nd(III), Gd(III), Sm(III), Pr(III), Tb(III), Dy(III), Eu(III), Lu(III), and Ce(III), with a concentration of 5 mmol) was introduced into a vigorously stirred ethanol solution (25 ml) containing the HBMT*p*BB ligand (15 mmol). The resulting reaction mixture underwent reflux for a duration of 5-10 hours to promote the interaction and formation of the desired complexes. Following this, the mixture was subjected to filtration, and the solvent was evaporated under vacuum conditions to reduce the volume by half.

The concentrated solution obtained from the solvent evaporation underwent further filtration and was subsequently rinsed with hot distilled water to remove any residual impurities. This thorough sequence of steps was meticulously executed to ensure the successful synthesis of the complexes involving lanthanide ions and the HBMT*p*BB ligand. The utilization of specific lanthanide salts in conjunction with the carefully controlled reaction conditions highlights the precision and systematic approach employed in the experimental process.

$$\textbf{3HBMT}\textit{p}\textbf{BB} \xrightarrow[\text{La(NO}_3)_3]{\text{Refluxed 7-9h}} \textbf{Ln(BMTpBB)}_3$$

Scheme-II: Preparation of metal complexes of benzilmonoximethiocarbohydrazide-*p*-bromobenzaldehyde ligand

Biological activity:

The antibacterial properties of both the ligand and its derived complexes were systematically assessed by evaluating their bactericidal efficacy against four bacterial strains-two gram-positive species, *B. subtilis* (MCC 2010) and *S. aureus* (MCC 2408), as well as two gram-negative species, *P. aeruginosa* (MCC 2080) and *E. coli* (MCC 2412). This assessment was carried out utilizing the disc diffusion method, a widely recognized technique for evaluating the antimicrobial activity of chemical compounds [16-18].

To ensure standardized conditions, a final concentration of 5 mM for all chemicals, including the ligand and its complexes, was achieved by freshly synthesizing and dissolving them in ethanol. This meticulous preparation aimed at maintaining the integrity of the experimental setup and ensuring the accuracy of the results obtained. The bacterial cultures, representing both gram-positive and gram-negative strains, were cultivated on nutrient agar, providing a nutrient-rich medium conducive to bacterial growth.

The chosen bacterial strains are representative of both gram-positive and gram-negative categories, allowing for a comprehensive evaluation of the ligand and its complexes' broad-spectrum antibacterial effectiveness. The agar-plate method served as a reliable and standardized means to discern the inhibitory impact of these compounds on bacterial growth, contributing valuable insights into their potential as antimicrobial agents.

In vitro cytotoxicity

Employing the Meyer et al. technique [19], the cytotoxicity of both the synthesized Schiff base and its complexes with La(III), Nd(III), Gd(III), Sm(III), Pr(III), Tb(III), Dy(III), Eu(III), Lu(III), and Ce(III) was evaluated through a brine shrimp bioassay. The experimental setup involved the use of a shallow, rectangular plastic dish measuring 22 x 32 cm for hatching brine shrimp (Artemia salina leach) eggs. To create an artificial saltwater environment, double-distilled water was combined with a commercial salt solution. The plastic dish was partitioned unevenly using a perforated tool, with the larger compartment darkened and containing approximately 50 mg of eggs, while the smaller compartment was exposed to natural light.

After two days, the nauplius was extracted from the illuminated side using a pipette. For the preparation of the test substance, 20 mg of each chemical was dissolved in 2 ml of dimethylformamide (DMF). A reference vial, containing only 2 ml of DMF, was also preserved. From the stock solution, concentrations of 10-100 μg/ml were transferred to nine vials (with three vials for each dilution used per test sample, and the LD_{50} representing the mean of three values). The solvent was allowed to evaporate overnight. After two days when the shrimp larvae were ready, 1 ml of seawater and 10 shrimp (30 shrimp per dilution) were introduced into each vial, with the volume adjusted to 5 ml using seawater. The survival count was conducted 24 hours later, and LD_{50} values were calculated utilizing data analysis facilitated by a Finney computer program. This comprehensive methodology ensured a systematic and thorough assessment of the cytotoxic potential of the synthesized compounds and their complexes.

Results and discussion:

The molar conductance data in **Table 1** suggests that the Lanthanide(III) complexes are 1:1 electrolytic in nature [20]. The magnetic moments observed in these complexes show little departure from the Van-Vleck values, indicating a limited role of the *4f* electrons in bond formation.

Table 1: Analytical and physical data of the ligand and its lanthanide (III) metal complexes

Compound	Color	Yield %	M.P. / Dec. point°C	Elemental Analysis						Magnetic Moments (B.M.)	Electrical Conductance 10^{-3} M (nitrobenzene) Mhos
				% M Found (Calcd)	% C Found (Calcd)	% H Found (Calcd)	% N Found (Calcd)	% O Found (Calcd)	% Br Found (Calcd)		
HBMT*p*BB	Yellow	73.96	213	-	54.79 (55.01)	3.76 (3.78)	14.53 (14.58)	3.31 (3.33)	16.54 (16.63)	-	-
[Sm(BMT*p*BB)₃]NO₃	Green	70.74	293	9.01 (9.11)	47.90 (47.99)	3.06 (3.09)	13.44 (13.57)	5.75 (5.82)	14.33 (14.50)	1.56	25.14
[Nd(BMT*p*BB)₃]NO₃	Gray	55.77	301	9.91 (9.81)	52.20 (52.02)	3.36 (3.30)	14.76 (14.49)	6.33 (6.16)	6.33 (6.66)	3.58	21.91
[Pr(BMT*p*BB)₃]NO₃	Yellow	69.05	311	8.48 (8.59)	48.22 (48.26)	3.03 (3.11)	13.59 (13.65)	5.37 (5.85)	14.59 (14.60)	3.43	27.89
[Eu(BMT*p*BB)₃]NO₃	Gray	75.17	300	9.01 (9.20)	47.85 (47.94)	3.06 (3.09)	13.55 (13.56)	5.72 (5.81)	14.43 (14.50)	3.43	20.00
[Lu(BMT*p*BB)₃]NO₃	Yellow	74.15	308	10.34 (10.45)	47.27 (47.28)	3.01 (3.04)	13.34 (13.37)	5.71 (5.73)	14.21 (14.30)	-	30.82
[Ce(BMT*p*BB)₃]NO₃	Black	74.11	322	8.50 (8.54)	48.03 (48.29)	3.06 (3.11)	13.51 (13.66)	5.37 (5.85)	14.22 (14.60)	2.50	20.42
[La(BMT*p*BB)₃]NO₃	Green	79.32	293	8.75 (8.81)	50.07 (50.22)	3.19 (3.23)	13.21 (13.22)	3.03 (3.04)	14.91 (15.00)	-	23.35
[Dy(BMT*p*BB)₃]NO₃	Green	62.51	318	9.85 (9.93)	48.29 (48.40)	3.09 (3.12)	12.77 (12.84)	5.83 (5.86)	12.12 (12.16)	10.55	26.24
[Gd(BMT*p*BB)₃]NO₃	Brown	74.90	303	9.58 (9.64)	48.53 (48.56)	3.11 (3.13)	12.83 (12.88)	5.86 (5.89)	14.62 (14.73)	7.82	23.44
[Tb(BMT*p*BB)₃]NO₃	Yellow	76.49	302	9.48 (9.58)	47.69 (47.74)	3.05 (3.07)	13.43 (13.50)	5.70 (5.79)	13.62 (14.40)	9.54	23.33

Electronic absorption spectra:

Electronic frequencies, along with their tentative assignments for ligands and the corresponding Lanthanide(III) complexes, were recorded in both solid-state (diffused reluctance spectra) and solution-state (DMF). The data presented in **Table 2** indicates that the Nephelauxetic value, being less than unity, and positive values for all other parameters suggest some covalent character in the

metal–ligand bond. Notably, the value of ($b^{1/2}$) implies a comparative involvement of the 4f orbital in the metal–ligand bond. The observed trend reveals a decrease in covalence from Pr(III) to Sm(III) complexes, attributed to lanthanide contraction [21-23].

Table 2: Electronic absorption spectral data of HBMTpBB ligand and its Ln(III) metal complexes

Compound	λnm	ε (dm³/mol/cm)	Transition	
HBMH*p*CB	366	15068	$\pi \to \pi^*$	
	298	13513	$\pi \to \pi^*$	
	225	13581	$\pi \to \pi^*$	
[Sm(BMH*p*BB)₃]NO₃	662	856	$^6H_{5/2} \to {}^4G_{5/2}$	
	571	793	$^6H_{5/2} \to {}^4G_{7/2}$	$\beta_{ave} = 0.9971$,
	479	2136	$^6H_{5/2} \to {}^4I_{18/2}$	$\eta = 0.00003$,
	448	28398	$^6H_{5/2} \to {}^6P_{5/2}$	$b^{1/2} = 0.0030$,
	385	29656	$^6H_{5/2} \to {}^6G_{3/2}$	$\delta\% = 0.3075$
	375	28790	$^6H_{5/2} \to {}^9H_{9/2}$	
[Lu(BMH*p*BB)₃]NO₃	444	9865	MLCT	
	473	14338	MLCT	
	389	17688	MLCT	
[Ce(BMH*p*BB)₃]NO₃	310	17288	$^5F_5 \to {}^2D_{3/2}$	
	258	15336	$^5F_5 \to {}^2D_{5/2}$	
Eu(BMH*p*BB)₃]NO₃	579	920	$^5D_0 \to {}^7F_4$	
	466	13822	$^5D_0 \to {}^7F_3$	
	392	19782	$^5D_0 \to {}^7F_2$	$\beta_{ave} = 0.9887$, $\eta = 0.0057$, $b^{1/2} = 0.0952$, $\delta\% = 1.1438$
	258	29766	LMCT	
	2222	40080	LMCT	
Pr(BMH*p*BB)₃]NO₃	595	4178	$^3H_4 \to {}^1D_2$	$\beta_{ave} = 0.9914$, $\eta = 0.00434$, $b^{1/2} = 0.0657$, $\delta\% = 0.8707$
	485	7568	$^3H_4 \to {}^3P_0$	
[Nd(BMH*p*BB)₃]NO₃	873	136	$^4I_{9/2} \to {}^4F_{3/2}$	
	794	175	$^4I_{9/2} \to {}^4F_{5/2}$	
	736	201	$^4I_{9/2} \to {}^4F_{9/2}$	
	685	102	$^4I_{9/2} \to {}^4G_{5/2,}$	$\beta_{ave} = 0.9997$,
	579	198	$^4I_{9/2} \to {}^4G_{7/2}$	$\eta = 0.001518$,
	510	221	$^4I_{9/2} \to {}^4G_{9/2}$	$b^{1/2} = 0.0351$,
	458	725	$^4I_{9/2} \to {}^2P_{1/2}$	$\delta\% = 0.3040$
	438	879	$^4I_{9/2} \to {}^4D_{3/2}$	
	351	8137	$^4I_{9/2} \to {}^4D_{1/2}$	
	343	7042	$^4I_{9/2} \to {}^2G_{7/2}$	
[La(BMH*p*BB)₃]NO₃	415	19368	MLCT	
	349	21222	MLCT	
	370	26556	MLCT	
[Dy(BMTpBB)₃]NO₃	805	156	$^4H_{15/2} \to {}^6F_{5/2}$	
	753	315	$^4H_{15/2} \to {}^6F_{3/2}$	
	473	4098	$^4H_{15/2} \to {}^4F_{9/2}$	$\beta_{ave} = 0.9927$, $\eta = 0.0036$, $b^{1/2} = 0.0603$, $\delta\% = 0.732$
	452	4538	$^4H_{15/2} \to {}^4I_{15/2}$	
	425	7869	$^4H_{15/2} \to {}^4I_{3/2}$	
[Gd(BMH*p*BB)₃]NO₃	510	1363	LMCT	
	419	25568	LMCT	
[Tb(BMTpBB)₃]NO₃	624	1711	$^5D_4 \to {}^7F_3$	
	584	3489	$^5D_4 \to {}^7F_4$	$\beta_{ave} = 0.9958$, $\eta = 0.00208$, $b^{1/2} = 0.0455$, $\delta\% = 0.0049$
	545	5697	$^5D_4 \to {}^7F_5$	
	488	13984	$^5D_4 \to {}^7F_6$	

FT(IR) spectra:

The significant FT(IR) spectral bands of the HBMT*p*BB ligand, along with those of its trivalent lanthanide (III) metal complexes, are detailed in **Table 3**. Within this spectral analysis, the absence of the broad band observed at 3404 cm⁻¹, attributed to the oximino (-OH) group in the HBMT*p*BB ligand, in the lanthanide (III) metal complexes' spectra signifies the coordination of the HBMT*p*BB ligand to the metal ion through the deprotonation of the oximino group. In the FT(IR) spectrum of

the HBMT*p*BB ligand, distinct bands at 1609 and 1559 cm^{-1} are ascribed to the (>C=NN-) and (>C=NOH) groups, respectively. These bands exhibit a frequency shift towards lower values in the spectra of lanthanide (III) metal complexes, suggesting the coordination of the HBMT*p*BB ligand to the central lanthanide (III) metal ions through the oximino and azomethine nitrogens.

Furthermore, this coordination is substantiated by the emergence of new bands at 433-512 and 495-545 cm^{-1}, corresponding to the υ(M-S) and υ(M-N) bands, respectively, in all lanthanide (III) metal complexes. These spectral features provide additional support for the coordination mode of the HBMT*p*BB ligand, highlighting the interaction of the ligand's functional groups with the central lanthanide (III) metal ions. The comprehensive spectral analysis underscores the intricate nature of the metal-ligand coordination in these complexes.

Table 3: IR spectral bands of the ligand (HBMT*p*BB) and its metal complexes (cm^{-1}):

Assignments	HBMT*p*BB	Sm(III)	Pr(III)	Lu(III)	Eu(III)	Ce(III)	Nd(III)	La(III)	Dy(III)	Gd(III)	Tb(III)
νOH Oximino	3404	-	-	-	-	-	-	-	-	-	-
N-H	3290	3302	3282	3297	3202	3232	3187	3295	3297	3191	3301
νC=C Ar.	3235	3084	2921	3080	3191	3140	2915	3023	3080	2918	2936
νC=NN	1609	1638	1634	1588	1599	1578	1633	1577	1645	1599	1593
νC=NO	1559	1506	1558	1506	1492	1493	1417	1491	1506	1492	1487
νN-N	992	1057	1021	1056	1088	1133	1013	1119	1022	1022	1073
νN→O	-	914	968	957	928	1021	1056	1049	922	928	928
νM-N	-	545	524	533	518	530	562	514	495	522	522
νM→N	-	491	511	483	425	511	512	503	438	433	436

PMR spectra:

The PMR spectra of the unbound HBMTpBB ligand and its diamagnetic complex [Lu(BMTpBB)$_3$] were meticulously recorded in deuterated dimethyl sulfoxide (d$_6$-DMSO). In the free HBMT*p*BB ligand, a sharp singlet at δ11.59 ppm, attributed to the oximino protons, was evident. However, this characteristic band was notably absent in the [Lu(BMT*p*BB)$_3$] and [La(BMT*p*BB)$_3$] complexes, indicating the involvement of the oximino group in coordination through metal ions, as evidenced by the deprotonation of this group. Another singlet at δ9.00 ppm was identified as the azomethine proton of the HBMTpBB ligand and the Lu(III) and La(III) complexes. Within the aromatic region, a multiplet of proton signals was observed between 7.60 and 8.44 ppm for both the free HBMTpBB ligand and its Lu(III) and La(III) complexes. This consistent spectral pattern suggests the preservation of the aromatic structure in the ligand and its complex, affirming the structural integrity of the ligand upon coordination with Lu(III) ions. The detailed examination of the PMR spectra provides valuable insights into the coordination-induced changes in the chemical environment of protons, elucidating the nature of the metal-ligand interaction in the complex.

Powder X-Ray Diffraction study of ligand and its coordination complexes:

Since growing appropriate crystals for a complete X-ray investigation was not possible, X-ray diffraction tests of the powder sample were conducted. Powder XRD patterns of the HBMTpBB and its La(III), Nd(III), Gd(III), Sm(III), Pr(III), Tb(III), Dy(III), Eu(III), Lu(III), and Ce(III) complexes were recorded over the 2θ= 10º–90º range scanning angle. The diffractogram of both ligands was used to measure the observed interplanar spacing values ('d' in A°) with respect to main peaks with relative intensity at wavelength = 1.54060 (Cu K-alpha). The HBMTpBB ligand exhibited a diffractogram with sharp peaks designating their crystalline nature.

The complex of Pr(III) exhibited a diffractogram with sharp peaks designating the crystalline nature of the complex. All the other complexes, viz., La(III), Nd(III), Gd(III), Sm(III), Pr(III), Tb(III), Dy(III), Eu(III), Lu(III), and Ce(III) complexes, produced diffractogram having no well-defined crystalline peaks indicating that all these complexes are amorphous in nature.

Biological Activity Studies

The determination of minimum inhibitory concentrations (MICs) for both the HBMTpBB ligand and the [La(BMTpBB)$_3$]NO$_3$ complexes against gram-positive bacteria, namely *B. subtilis* (MCC 2010) and S. aureus (MCC 2408), as well as gram-negative bacteria *P. aeruginosa* (MCC 2080) and *E. coli* (MCC 2412), was conducted using a broth dilution assay to assess the antimicrobial activity of the synthesized compounds. The antibacterial results of the series revealed notable efficacy, with the [Gd(BMTpBB)$_3$]NO$_3$ complex demonstrating high activity, and the [Ce(BMTpBB)$_3$]NO$_3$ complex exhibiting good activity against gram-positive organisms. Conversely, the [Dy(BMTpBB)$_3$]NO$_3$ and [La(BMTpBB)$_3$]NO$_3$ complexes displayed good activity against gram-negative organisms. The remaining compounds demonstrated moderate to good antibacterial activity. Comparative standard such as *streptomycin* was employed in these assessments.

Furthermore, each prepared compound underwent efficacy testing against three common types of fungi-*C. albicans*, and *S. cerevisiae*. Among the compounds, the [Ce(BMTpBB)$_3$]NO$_3$ and [Dy(BMTpBB)$_3$]NO$_3$ complexes emerged as the most effective against both types of fungi, while the remaining compounds exhibited only mild antifungal activity. The benchmark antifungal standard, fluconazole, was used for comparative analysis. These findings collectively underscore the diverse and promising antimicrobial activities of the synthesized compounds against both bacteria and fungi, providing valuable insights for potential therapeutic applications.

Table 4: Antimicrobial activities of the ligand (HBMTpBB) and its metal complexes (mm)

| Assignments	*B. subtilis*	*P. aeruginosa*	*S. aureus*	*E. coli*	*C. albicans*	*S. cerevisiae*
HBMTpBB	10	0	15	14	11	12
[Sm(BMTpBB)$_3$]NO$_3$	9	0	8	11	0	7
[Nd(BMTpBB)$_3$]NO$_3$	12	0	8	9	7	6
[Pr(BMTpBB)$_3$]NO$_3$	8	0	0	12	10	6
[Eu(BMTpBB)$_3$]NO$_3$	0	0	0	15	6	0
[Lu(BMTpBB)$_3$]NO$_3$	0	0	0	12	7	8
[Ce(BMTpBB)$_3$]NO$_3$	0	0	0	17	10	10
[La(BMTpBB)$_3$]NO$_3$	9	12	10	10	6	8
[Dy(BMTpBB)$_3$]NO$_3$	10	13	9	14	10	9
[Gd(BMTpBB)$_3$]NO$_3$	11	12	8	10	9	8
[Tb(BMTpBB)$_3$]NO$_3$	8	7	6	8	7	7

In vitro cytotoxicity:

Only compounds containing Yb(III), Sm(III) and Ce(III) demonstrated moderate cytotoxic effects against *A. salina* in the context of cytotoxic activity. Conversely, the remaining compounds exhibited high LD$_{50}$ values, signifying a lack of cytotoxicity in these instances.

Table 5: Cytotoxic bioassay of HBMTpBB ligand and its metal complexes

Compound	LD$_{50}$ (µg/ml)
HBMTpBB	140
[Tb(BMTpBB)$_3$]NO$_3$	125
[Er(BMTpBB)$_3$]NO$_3$	135
[Eu(BMTpBB)$_3$]NO$_3$	140
[Yb(BMTpBB)$_3$]NO$_3$	110
[Lu(BMTpBB)$_3$]NO$_3$	100
[Ce(BMTpBB)$_3$]NO$_3$	90
[Tm(BMTpBB)$_3$]NO$_3$	125
[La(BMTpBB)$_3$]NO$_3$	130
[Pr(BMTpBB)$_3$]NO$_3$	125
[Sm(BMTpBB)$_3$]NO$_3$	110

Conclusion:

The geometry, physicochemical characteristics, and spectral data of the HBMT*p*BB ligand, as well as the lanthanide (III) ions, indicate the formation of complexes involving nitrogen atoms of amine, oxygen, and sulfur atoms of the higher carbohydrazide group. The trinuclear lanthanide (III) complexes formed with the HBMT*p*BB ligand exhibit a consistent 1:3 metal-to-ligand ratio. Notably, all the prepared complexes of the HBMT*p*BB ligand adopt a seven-coordinate geometry, aligning with the proposed structure for efficient lanthanide (III) complexes. This conformity in the results underscores the successful synthesis of the complexes and supports the envisioned structural arrangement for these lanthanide (III) complexes.
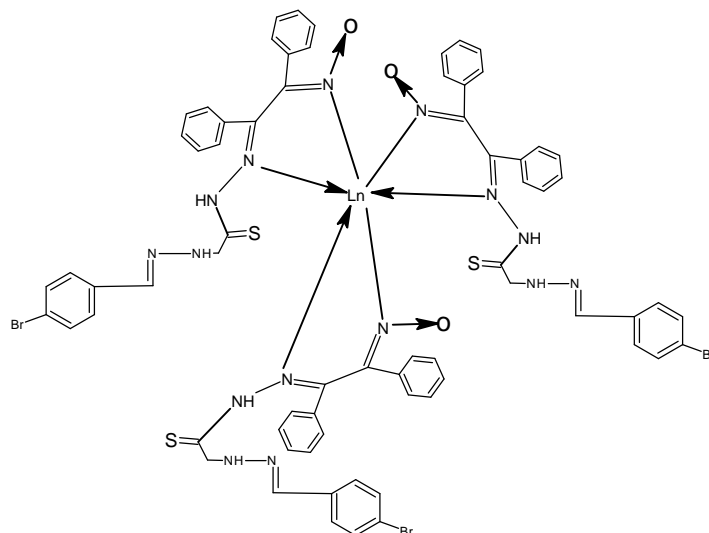
Where: Ln = La(III), Nd(III), Gd(III), Sm(III), Pr(III), Tb(III), Dy(III), Eu(III), Lu(III), and Ce(III)

References:
1. Abdel Rahman.D E., Mohamed.K O. (2014). Synthesis of novel 1,3,4-thiadiazole analogues with expected anticancer activity, Der Pharma Chemica, 6(1), P: 323- 335.
2. Ansari K F., Lal. C. (2009). Synthesis and biological activity of some heterocyclic compounds containing benzimidazole and beta-lactam moiety, J. Chem. Sci., Vol. 121, No.6, 1017-1025.
3. Azarifar. D., Shaebanzadeh.M. (2002). Synthesis and characterisation of new 3, 5-dinaphthyl substituted 2- pyrazolines and study of their antimicrobial activity, Molecules, 7, 885-895.
4. Bheru S.K., Man S. (2014). Synthesis, characterisation, antibacterial, antioxidant, DNA binding and SAR study of a novel pyrazine moiety bearing 2-pyrazoline derivatives, New J. Chem., 38, 4290-4299.
5. Fatondji.H.R.,Gbaguidi.F.,Kpoviessi.S.,Bero.J.,Hannaert.V.,QuetinLeclercq.J.,Poupaert.J.,Mou dachirou.M.,Acc rombessi.G.C. (2011). Synthesis, characterisation and trypanocidal activity of some aromatic thiosemicarbazones and their 1,3,4-thiadiazolines derivatives, African Journal of Pure and Applied Chemistry, Vol. 5(1), p:59-64.
6. Francis A.G., Robert M.G. (2011). Organic Chemistry, 8th edition, MeGraw-Hill Comparies, Inc, pp:880.
7. Jumbad H. T., Mustafa S. K., Ammar H. A. (2014). Synthesis and characterisation of novel Schiff bases containing pyrimidine unit, Arabian Journal of Chemistry, 7, P:157-163.
8. Manjula.P.S., Sarojini.B.K., Darshan Raj.C.G. (2015). Antibacterial and in vitro antioxidant activities of some 4 4-amino-1,2,4-triazole-5(4h)-thione derivatives, J Fundam appl Sci., 7(3), 394-407.
9. Nitulescu.G.M., Draghici.C.,Olaru.O.T. (2013). New Potential Antitumor Pyrazole Derivatives: Synthesis and Cytotoxic Evaluation, Int. J. Mol. Sci. , 14, 21805-21818.
10. Noto R., Buccheri F ., Cusmano G ., Gruttadauria M ., Werber G. (1991). Substituent effect on oxidative cyclisation of aldehyde thiosemicarbazones with ferric chloride, J. Heterocyclic Chemistry, 28, 1421.
11. Nandal P, Kumar R, Khatkar A, Khatkar SP, Taxak VB. Synthesis, characterisation, enhanced photoluminescence, antimicrobial and antioxidant activities of novel Sm(III) complexes containing 1-(2-hydroxy-4,6-dimethoxyphenyl)ethanone and nitrogen-containing ancillary ligands. J Mater Sci Mater Electron. 2016;27(1):878.
12. Sosnovskikh V. Synthesis and reactions of halogen-containing chromones. Russ Chem Rev. 2003; 72(6):489.
13. Meyer B. N., Ferrigni N. R., Putnam J. E., Jacobsen L. B., Nichols D. E., McLaughlin J. L., Planta Med. 45 (1982) 31.
14. Sharma A and Shah M; Synthesis and characterisation of some transition metal complexes derived from bidentate Schiff base ligand; *J of Appl Chem;* **2013**, 3(5), 62-66.
15. Kido, Takafumi; Ikuta, Yuichi; Sunatsuki, Yukinari; Ogawa, Yoshihiro; Matsumoto, Naohide; Re, Nazzareno (2003). Nature of Copper(II)−Lanthanide(III) Magnetic Interactions and Generation of a Large Magnetic Moment with Magnetic Anisotropy of 3d−4f Cyclic Cylindrical Tetranuclear Complexes; Inorganic Chemistry, 42(2), 398–408.
16. Maurya R.C. et al; Synth and React in Inorg and Metal Chem; 2003, 33(5), 801-816.
17. Connie L; Chem Sci; 2019, 1-20.
18. Sheto S. M. et al; The Royal Soc of Chem; 2020, 10(10), 5853-5863.
19. Thiakou K. A, et al.; Polyhedron; 2006, 25, 2869-2879.
20. Tondon S P and Mehta P C, *J Chem Phys*., 1970, **52**, 4314.
21. Bootwala S; Novel binuclear copper(II) complexes of tetradentate (N, N, N, N) functionalised ligands Synthesis and characterisations; *IJIRSET*; **2016,** 5(3), 2823-2829.
22. Nemade A, Patil K and Kolhe V; Synthesis, composition and spectral studies of some transition metal complexes with 3-aminolawsonoxime; *Res J Chem Sci;* **2017**, 7(1), 25-31.

23. Al-Hamdani A, Mahmoud M and Bakir S; Synthesis, structural studies of some new transition metals complexes of semicarbazide hydro-chloride Schiff base derivatives; **2013**, 1(3), 583-596.

24. Alsaygh A, Al-humid J and Najjar I; Iridium (III) hydrocyclometallated-imine complexes, as a result of C-H bond activation in coordinated ligand, spectroscopic studies; *Asian J of Sci and Tech;* **2014**, 5(11), 647-652.

25. Sankhe S and Kamble P; Synthesis and characterisation of Pd(II), Zn(II), Cd(II) and Hg(II) metal coordination compounds of (4-(dimethylaminobenzylidene) hydrazono)butane-2-one oxime; *JETIR*; **2018**, 5(8),677-682.